Chemical Engineering Science ▮ (▮▮▮▮) ▮▮▮–▮▮▮

Contents lists available at ScienceDirect

Chemical Engineering Science

journal homepage: www.elsevier.com/locate/ces

Application of power addition as modelling technique for flow processes: Two case studies

Pierre de Wet [a,*], J. Prieur du Plessis [b], Sonia Woudberg [b]

[a] Council for Scientific & Industrial Research (CSIR), PO Box 320, Stellenbosch 7599, South Africa
[b] Applied Mathematics Division, Department of Mathematical Sciences, University of Stellenbosch, Private Bag X1, Matieland 7602, South Africa

ARTICLE INFO

Article history:
Received 6 August 2010
Received in revised form
17 December 2010
Accepted 20 January 2011

Keywords:
Fluidisation
Mathematical modelling
Non-Newtonian fluids
Packed bed
Porous media
Slurries

ABSTRACT

In many of the continuum processes typically found in chemical engineering, the functional dependency of the dependent variable is only known for large and small values of the independent variable. Exact solutions in the transitional regime are often obscure for various reasons (e.g. narrow band within which the transition from one regime to the other occurs, inadequate knowledge of the physics in this area, etc.). An established method for the matching of limiting solutions is reviewed and subsequently applied. The method regards the known solutions as asymptotes and proposes addition to a power of such asymptotes. It yields a single, adjustable correlating equation that is applicable over the entire domain. This procedure circumvents the introduction of *ad hoc* curve fitting measures for the different regions and subsequent, unwanted discontinuities in piece-wise fitted correlative equations for the dependent variables. Experimental data of two diverse processes, namely flow in a straight-through diaphragm valve and the fluidisation of a packed bed, are analysed as case studies. Empirical results are investigated for possible asymptotic bounds whereafter power addition is applied to the functional dependencies. The outcome is compared to those of the empirical models and the results discussed. The procedure is revealed to be highly useful in the summarising and interpretation of experimental data in an elegant and simplistic manner. It may also, in general, aid the setup of experimental apparatus for investigation of continuum processes.

1. Introduction

The dependence of modern chemical engineering research on precise, credible experimental practices is undeniable. The empirical equations derived from these investigations impart understanding of the underlying physics are crucial for the development of computational routines and form an integral part of the design process. It is common practice to represent the general trend in a set of collected data by drawing a line through the individual datum points on the plot. Correlation between the drawn predictive curve and the data is then evaluated against some norm. Although theoretical knowledge of the functional behaviour is helpful it is not a prerequisite for the construction of graphical correlation and a curve best suited to the particular problem is chosen. The better the predictive curve on the graphical presentation corresponds to the physical reality, the greater the accuracy is with which the curve's functional expression will predict physical trends.

Knowledge of the asymptotic behaviour (traits at extreme values of the independent variable) of the dependent variable may often be used to glean information about the process as a whole. One such method, in use for some time especially in engineering practice, has been to simply match the asymptotic conditions by straightforward addition of the respective expressions. In so doing a single relation is obtained that is supposed to hold over the entire domain of the independent variable. Frequently, however, intermediate values do not lie on this matched solution. ~~In~~ Churchill and Usagi (1972) formalised a method that not only combines the solutions at extremal values into a single expression, but also yields close correlation in the transitional zone between the extremities. In the aforementioned article and subsequent work (Churchill and Usagi, 1972, 1974; Churchill, 1988, 2001) the use and wide application possibilities of the method and its variations were accentuated. Their method, which yields an equation of simple, elegant form that interpolates between limiting solutions, is applicable to phenomena which vary uniformly between known, limiting solutions and is especially useful for the evaluation and summarising of experimental and computational data. Furthermore, it is particularly convenient for design purposes as it renders an expression that holds true over the entire domain of the dependent variable and has the same form for all correlations. Whether it presents an exact

* Corresponding author. Tel.: +27 21 888 2569; fax: +27 21 888 2693.
E-mail addresses: pdwet@csir.co.za (P. de Wet), woudberg@sun.ac.za (S. Woudberg).

0009-2509/$ - see front matter © 2011 Published by Elsevier Ltd.
doi:10.1016/j.ces.2011.01.040

Please cite this article as: de Wet, P., et al., Application of power addition as modelling technique for flow processes: Two case studies. Chemical Engineering Science (2011), doi:10.1016/j.ces.2011.01.040

representation of the transfer process cannot be proven scientifically, yet the method is widely applicable and accepted.

In the present work the general method proposed by Churchill and Usagi is applied to collected experimental data for two diverse chemical engineering processes: flow in a straight-through diaphragm valve (De Wet, 2010); and the fluidisation of a packed bed (De Wet et al., 2009). Different scenarios of the limiting functions and or values are investigated. Curve adjustment and the importance of the point of intersection of asymptotes on obtained results are discussed.

2. Power addition as curve fitting technique

This section presents a condensed outline of the method thoroughly described by Churchill and Usagi (1972, 1974) and Churchill (1988, 2001, 1974).

Chemical engineering processes, such as momentum and thermal transfer processes, are often expressed in terms of a continuum process. In many of these instances the value of a sought after parameter is expressible as a function of certain known parameters at low and high values. These limiting solutions for large and small values of the independent variables may be regarded as asymptotic conditions of the dependent variable. Power addition of expressions valid for two opposing ranges is a procedure used to produce a combined result which is valid for both of these ranges. Since each of the limiting expressions predominates in their respective regions of applicability, a unified model can be obtained using such a technique.

Often the functional expression of the dependent variable is in the form of a power dependency upon some independent variable, x. Suppose the functional dependence, f, of such a process is described by (Churchill and Usagi, 1972, 1974)

$$f \to f_0\{x\} = Ax^{\alpha} \quad \text{as } x \to 0, \tag{1}$$

$$f \to f_\infty\{x\} = Bx^{\beta} \quad \text{as } x \to \infty, \tag{2}$$

where Eqs. (1) and (2) denote the functional expressions at the lower and upper extremal values of x, respectively. Frequently, however, the values of the dependent variable at the transition between the asymptotic extremities do not lie exactly on a matched solution. This is due to the cross-over 'rate' between the two asymptotic processes. Churchill and Usagi (1972, 1974) and Churchill (1988, 1974) demonstrated that the use of power addition, the most general forms of which are given by

$$f^s\{x\} = [(Ax^{\alpha})^s + (Bx^{\beta})^s], \tag{3}$$

or

$$f\{x\} = [(Ax^{\alpha})^s + (Bx^{\beta})^s]^{1/s}, \tag{4}$$

may lead to dramatic improvement in correlation with experimental data. It is important to note that the explicit expression of the asymptotes in terms of a power dependency is not permutable. In other words, in the present study the lower asymptote will always be associated with coefficient A and exponent α; the upper with B and β.

By adjusting the value of the exponent, s, the curve may be shifted so as to more closely trace the expected or empirical values, yielding better correspondence between predictive equation and experimental results for a particular process. The higher the value of $|s|$, the more closely the solution traces the asymptotic expressions, i.e. the more abrupt the transition. Conversely, a gradual change-over between extremal solutions will signify that a small $|s|$ should be used. Hence, s is indicative of the rate of transition between the constituent predictive equations.

2.1. Increasing dependence

When the dependent variable is an increasing power of the independent variable, in other words if the power of x in Eq. (3) is greater at the higher limit, that is

$$\alpha < \beta, \tag{5}$$

the expression

$$f\{x\} = [f_0^s\{x\} + f_\infty^s\{x\}]^{1/s}, \tag{6}$$

is usually desirable for interpolation between the extremal values.

Theoretically the matched function in Eq. (6) will have no upper bound and will only be bounded from below by the functional expression for small values of x, i.e the term Ax^{α} in Eq. (3) will form a lower bound on the values that the independent variable may take on. The arbitrary exponent s will in this case have a positive value.

2.2. Decreasing dependence

Should the dependence of $f\{x\}$ decrease with an increase in the independent variable, i.e.

$$\alpha > \beta, \tag{7}$$

in Eq. (3), two possibilities exist: the asymptotes may either together determine (a) the lower bound; or (b) the upper bound of the resulting matched curve. Knowledge of the process being modelled and/or experimental data will be indicative of the particular case.

2.2.1. Bounded from below

Decreasing dependence upon the independent variable is such that the solutions for extremal values, i.e. the functional expressions for the asymptotes, bind all possible solutions to the process from below. Suppose, for the sake of an illustrative example, that the limiting solutions to such a process are given by the simple relations

$$f \to f_0\{x\} = \frac{1}{x} \quad \text{as } x \to 0, \tag{8}$$

$$f \to f_\infty\{x\} = 1 \quad \text{as } x \to \infty. \tag{9}$$

This corresponds to Eqs. (1) and (2) with coefficients $A=1$, $B=1$ and exponents, $\alpha=-1$ and $\beta=0$. The matched solution, raised to the shifting exponent will thus be

$$f\{x\} = \left[\left(\frac{1}{x}\right)^s + 1\right]^{1/s}. \tag{10}$$

2.2.2. Bounded from above

The asymptotes, $f_0\{x\}$ and $f_\infty\{x\}$, of the process being modelled form an upper bound on the possible values that the function can assume. Consider, as an example, the very simple case in which the asymptotes constituting the matched equation are given by

$$f \to f_0\{x\} = x \quad \text{as } x \to 0, \tag{11}$$

$$f \to f_\infty\{x\} = 1 \quad \text{as } x \to \infty. \tag{12}$$

To ensure that the matched solution approaches the limiting functions from below, the shifting exponent now needs to take on a negative value. However, the obtained curve will still approach the asymptotes as $|s|$ increases. The introduction of a negative value for s may be circumvented by taking the reciprocal of the

Please cite this article as: de Wet, P., et al., Application of power addition as modelling technique for flow processes: Two case studies. Chemical Engineering Science (2011), doi:10.1016/j.ces.2011.01.040

original dependent variable, i.e. by defining

$$\frac{1}{g\{x\}} = \frac{1}{Ax^{\alpha}} + \frac{1}{Bx^{\beta}} = \frac{1}{g_0\{x\}} + \frac{1}{g_{\infty}\{x\}}, \tag{13}$$

before it is raised to s, ensures that $s > 0$.

2.3. Crossing of one limiting solution

In some phenomena the process is not bound completely by the limiting solutions and one of the limiting functions may be crossed as the solution approaches it. Although it is presumed that both the lower functional dependency, $f_0\{x\}$, and the upper limiting value, $f\{\infty\}$, are known, Eq. (3) is not directly applicable, since for any positive values of the shifting exponent, Eq. (3) gives values that fall above $f_0\{x\}$ and $f\{\infty\}$ (see Sections 2.1 and 2.2.1). In cases such as these a function is postulated viz.,

$$f_{\infty}\{x\} \to f\{\infty\} \quad \text{as } x \to \infty, \tag{14}$$

which not only forms an upper bound on attainable values of the dependent variable, but also approaches the limiting value from above. Using a function of the form (Churchill and Usagi, 1972, 1974),

$$f_{\infty}\{x\} = f\{\infty\}\left[1 + \left(\frac{x_A}{x}\right)^{\alpha}\right], \tag{15}$$

instead of $f\{\infty\}$, solves this problem, since as $x \to \infty$ the second term in square brackets on the right hand side of Eq. (15) approaches zero (provided that $\alpha \geq 0$).

Constructing a new dependency of the form suggested by Eq. (3), with $g\{x\} = 1/f\{x\}$, $g_0\{x\} = 1/f_0\{x\}$ and $g_{\infty}\{x\} = 1/f_{\infty}\{x\}$, with $f_{\infty}\{x\}$ the newly defined relation of Eq. (15), yields

$$\left(\frac{f_0\{x\}}{f\{x\}}\right)^s = 1 + \left(\frac{f_0\{x\}}{f\{\infty\}\left[1 + \left(\frac{x_A}{x}\right)^{\alpha}\right]}\right)^s, \tag{16}$$

after simplification. An example of the family of curves obtained through the procedure outlined above is illustrated in Fig. 1. To show the influence of a change in the value of the shifting exponent upon the obtained solution a few selected values of s were plotted: a low s-value implies gradual transition with the change-over becoming more abrupt as s is increased. A function of the form of Eq. (15), with $x_A = 5$ and $\alpha = 2$ kept constant (allocated values selected purely for demonstrative purposes), was utilised to approximate the upper limit. Investigation of the influence of the arbitrary constant, x_A, and arbitrary exponent, α, in Eq. (16) showed that the former adjusts the point of intersection of the newly defined function, f_{∞}, with f_0, while the latter alters its curvature.

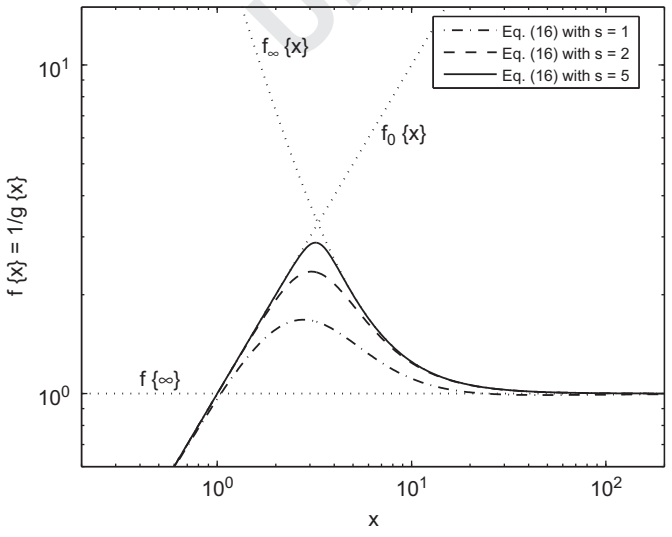

Fig. 1. Application of power addition when the solution crosses one of the limiting functions. The effect on the matched solution for selected values of the shifting exponent, s, is demonstrated.

2.4. Critical point and shifting exponent

The *central* or *critical* point, x_c, of the matching curve is the value of the independent variable at which the asymptotes meet. Since the asymptotes intersect at this point, the numerical value of their respective functional expressions must be equal, that is

$$f_0\{x_c\} = f_{\infty}\{x_c\}. \tag{17}$$

As both functions, f_0 and f_{∞}, contribute equally to the added solution at this point, the resultant curve is most sensitive to variations in the value of the shifter, s, in the vicinity of x_c. Furthermore the maximal fractional deviation of the matched solution from either of the limiting solutions or asymptotic values will occur at precisely this point. Thus, from Eq. (17) it follows that

$$f^s\{x_c\} = f_0^s\{x_c\} + f_{\infty}^s\{x_c\} = 2f_0^s\{x_c\} = 2f_{\infty}^s\{x_c\}, \tag{18}$$

whence

$$\left(\frac{f\{x_c\}}{f_{\infty}\{x_c\}}\right)^s = \left(\frac{f\{x_c\}}{f_0\{x_c\}}\right)^s = 2. \tag{19}$$

The value of s may now be determined straightforwardly from Eq. (19) as

$$s = \frac{\ln 2}{\ln f\{x_c\} - \ln f_{\infty}\{x_c\}} = \frac{\ln 2}{\ln f\{x_c\} - \ln f_0\{x_c\}}. \tag{20}$$

In performing an experiment, it is therefore advantageous to arrange the physical conditions in such a manner that the independent variable is in close vicinity of x_c. Whenever the experimental value of $f\{x_c\}$ is known, one may proceed to determine the value of the shifter by Eq. (20). Alternatively, visual inspection by trial and error adjustment of the correlation between the predictive curve and data points may lead to an assignment of a value to s. As noted by Churchill and Usagi (1972) the matched curve is relatively insensitive to small variations in s. The required accuracy is determined by considerations such as the process involved, tunability of other parameters and allowable error-margin.

The following two sections involve application of the theory, outlined above, to two specific case studies.

3. Flow in straight-through diaphragm valves

Diaphragm valves possess several advantages that lead to their extensive use in diverse industrial applications. There are two types of diaphragm valves: the weir type used in piping systems that carry less viscous fluids; and the straight-through type suited to slurries and suspensions (Myles, 2000). The data sets of Mbiya (Mbiya, 2007; Fester et al., 2007), on which the current work is based, is concerned with the latter type of valve. Despite the broad scope of their use, only a few studies dealing with valve openings of aperture less than unity is available in the literature (Mbiya, 2007; Mbiya et al., 2009), hence the scarcity of other experimental data. The study of Mbiya supplied supplementary data sets and is an attempt at improving the prediction of the pressure losses through these valves.

The addition of a component, such as a valve, to a piping system leads to a local constriction (or dilation) of the cross-sectional area

Please cite this article as: de Wet, P., et al., Application of power addition as modelling technique for flow processes: Two case studies. Chemical Engineering Science (2011), doi:10.1016/j.ces.2011.01.040

and consequently also to a change in the flow path. Initially, at low Reynolds numbers the streamlines will trace out the irregular geometry caused by the valve's presence. While still in the laminar flow regime, an increase in Reynolds number will lead to the gradual development of localised areas of recirculation within the indentations of the diaphragm until, at turbulent flow conditions, the streamlines bypass these areas altogether. This is an intuitive explanation accounting for the constant resistance coefficients (pressure loss) obtained at high Reynolds numbers as reflected in the data (Mbiya, 2007; Fester et al., 2007; Mbiya et al., 2009). The aim of Mbiya's (Mbiya, 2007; Fester et al., 2007; Mbiya et al., 2009) experimental investigation was to more accurately predict the additional pressure loss incurred (i.e. the pressure loss coefficient), for four different opening positions, once a pipe had been fitted with a straight-through diaphragm valve.

3.1. Choice of Reynolds number

Often the relation between the shear rate, dv_x/dy, and shear stress, τ, of a non-Newtonian fluid is described by the power dependency,

$$\tau = K\left(-\frac{dv_x}{dy}\right)^n, \tag{21}$$

where K is the fluid consistency index and n the flow behaviour index (Streeter, 1966). Fluids exhibiting such behaviour are called power-law fluids. Depending on the value of the flow behaviour index, power-law fluids are classified into three broad groups: pseudo-plastic fluids if $n<1$; Newtonian fluids for $n=1$; and dilatant fluids for $n>1$. A true plastic substance has an initial yield stress that needs to be overcome before it assumes fluid-like properties, i.e. continuous deformation when subjected to a (further) shear stress (Streeter, 1966). The constitutive equation for the yield pseudo-plastic model can thus be formulated as

$$\tau = \tau_y + K\left(-\frac{dv_x}{dy}\right)^n, \tag{22}$$

with τ_y denoting the yield stress. Setting $n=1$ in Eq. (22) yields the so-called Bingham-plastic model, while $\tau_y=0$ results in it reverting back to that for power-law fluids, Eq. (21).

The Slatter–Reynolds number, Re_3, is based on the yield pseudo-plastic model and starts from the assumption that, in the presence of a yield stress, the core of the fluid moves as a solid, unsheared plug (Fester et al., 2007; Slatter, 1999), resulting in annular flow. It can be expressed as (Slatter, 1994)

$$Re_3 = \frac{8\rho\bar{v}_{\text{ann}}^2}{\tau_y + K\left(\frac{8\bar{v}_{\text{ann}}}{D_{\text{shear}}}\right)^n}. \tag{23}$$

In Eq. (23) $\bar{v}_{\text{ann}}$ denotes the corrected mean velocity in the annulus and D_{shear} the sheared diameter.

3.2. Empirical correlation

The *two-constant*, empirical model proposed by Mbiya (Mbiya, 2007; Fester et al., 2007; Mbiya et al., 2009) is based on a large set of accrued experimental data. The test rig consisted of pipes of different diameters (40, 50, 65, 80 and 100 mm), each of which was fitted with a diaphragm valve of similar diameter. The test fluids carboxymethyl cellulose (CMC) (at 5% and 8% concentration), glycerine or glycerol (concentrations of 75% and 100%), kaolin (a claylike mineral, at 10% and 13% concentrations) and water were, in turn, pumped through the pipes. Four different valve opening positions (25%, 50%, 75% and 100% open) were selected and the pressure drop in the pipe was recorded. The aim was to predict the pressure loss coefficient, $k_v\{Re_3\}$, for straight-through diaphragm valves. Mbiya (Mbiya, 2007; Fester et al., 2007; Mbiya et al., 2009) concludes by summarising his model, as being applicable to all sizes of valves tested, with the pressure loss coefficient given by

$$k_v = \begin{cases} \dfrac{1000}{Re_3}, & Re_3 < 10, \\ \dfrac{C_\Omega}{\sqrt{Re_3}\theta^2} + \dfrac{\lambda_\Omega}{\theta^2}, & Re_3 \geq 10. \end{cases} \tag{24}$$

Here C_Ω is a newly introduced model parameter or constant (Mbiya, 2007; Mbiya et al., 2009), inserted to facilitate proper agreement in the transitional region between the experimental data and correlative equation (24). The nominal turbulent loss coefficient is denoted by λ_Ω, while θ is the partial valve opening coefficient as ratio of the fully opened position, i.e. $\theta=0$ for a closed valve and $\theta=1$ for a fully opened valve. Note, however, that a fully opened valve does not correspond to an open tube flow condition.

Unfortunately, as can be seen in Eq. (24), to obtain good agreement with experimental results, an 'if'-condition and additional term had to be introduced at a Slatter–Reynolds number of 10. The two different solutions on either side of this value lead to an unwanted jump in the values of the dependent variable, i.e. the predicted cross-over at this Reynolds number is not smooth and contradicts the expected, intuitive-orderly behaviour of such a continuum transfer process.

3.3. Applying power addition

Regarding Eq. (24) in the limit where $Re_3\to\infty$, it is clear that $k_v\to\lambda_\Omega/\theta^2$. Hence, λ_Ω/θ^2 may be regarded as an asymptotic lower bound on k_v. Inspection of Mbiya's proposal thus evidently leads to the following definitions:

$$k_0 \equiv \frac{1000}{Re_3} \quad \text{for } Re_3\to 0, \tag{25}$$

and

$$k_\infty \equiv \frac{\lambda_\Omega}{\theta^2} \quad \text{for } Re_3\to\infty. \tag{26}$$

The direct addition of these results, $k_v = k_0 + k_\infty$, is then considered as a matching between the two asymptotic conditions, yielding a single solution, namely $k_v = 1000/Re_3 + \lambda_\Omega/\theta^2$, that covers the entire range of Reynolds numbers. Instead of the direct addition of the two asymptotes, power addition may now be applied to the asymptotic expressions, yielding

$$k_v^s = k_0^s + k_\infty^s, \tag{27}$$

which may be normalised to obtain

$$\frac{k_v}{k_\infty} = \left[\left(\frac{k_0}{k_\infty}\right)^s + 1\right]^{1/s}. \tag{28}$$

Instead of dividing Eq. (27) by k_∞, one may alternatively have chosen to designate k_0 as denominator. An extremely useful consequence of this type of modelling is the direct possibility of non-dimensionalisation.

Determination of the critical point and the value of the shifting exponent may now be performed in the manner outlined in Section 2.4. The critical point will thus be where

$$k_0 = k_\infty, \tag{29}$$

i.e.

$$\frac{1000}{Re_{3,c}} = \frac{\lambda_\Omega}{\theta^2}, \tag{30}$$

Please cite this article as: de Wet, P., et al., Application of power addition as modelling technique for flow processes: Two case studies. Chemical Engineering Science (2011), doi:10.1016/j.ces.2011.01.040

whence

$$Re_{3,c} = \frac{1000\theta^2}{\lambda_\Omega}, \tag{31}$$

where $Re_{3,c}$ denotes the Slatter–Reynolds number at the critical point. Since both λ_Ω and θ are constants for a given pipe diameter and valve opening, the Slatter–Reynolds number at which the critical point is to be found may easily be determined. The pressure loss coefficient at the critical point is thus given by $k_{v,c}=k_v\{Re_{3,c}\}$, the corresponding functional value obtained by using Eq. (31).

The preceding discussion of Section 2.4, cf. Eq. (20), now yields a value for the shifting exponent at the critical point, i.e.

$$s = \frac{\ln 2}{\ln k_{v,c} - \ln k_{\infty,c}} = \frac{\ln 2}{\ln k_{v,c} - \ln k_{0,c}}, \tag{32}$$

or in explicit form as

$$s = \frac{\ln 2}{\ln k_v(Re_{3,c}) - \ln\left(\frac{\lambda_\Omega}{\theta^2}\right)} = \frac{\ln 2}{\ln k_v(Re_{3,c}) - \ln\left(\frac{1000}{Re_{3,c}}\right)}. \tag{33}$$

Traversal of the data sets in search of the Re_3-value closest to those obtained by Eq. (31) may now be effected, the objective being to find the corresponding value of the dependent variable, $k_{v,c}$, at this point. Substituting these values into Eq. (33) will then yield a possible value for the shifting exponent. However, the datum point chosen may be a poor choice (an outlier, the result of a poor reading, etc.) and grounding the s-value solely on this one, single reading may lead to erroneous results. It is therefore recommended that the value of the intersection of the asymptotes be determined beforehand and the bulk of experimentation conducted in the area of the yielded independent variable, i.e. $Re_{3,c}$. In so doing a more accurate prediction will be obtained (from averaging numerous data points) and the fractional deviation of the matched solution from either of the limiting solutions or asymptotic values minimised. It is nevertheless important to note that the method is still an empirical one, based on experimental results, the wish being for an analytical expression in which this shifting exponent is linked to some quantifiable parameter in the process under consideration.

Since Mbiya's experimental readings were not arranged in such a manner as to focus on the transitional area between the asymptotes, the aforementioned methodical approach could not be used. In lieu, to circumvent the shifting exponent being based on an incorrect or inaccurate reading, a trial-and-error graphical approach was used. In Fig. 2 the data of one experimental setup, that of a pipe with internal diameter of 40 mm and a valve opening of 25%, have been plotted for illustrative purposes. Also in this figure is shown the empirical model of Mbiya (Mbiya, 2007; Fester et al., 2007; Mbiya et al., 2009), Eq. (24) and the solution obtained after application of power addition, Eq. (28). Two different values, namely 0.4 (solid curve) and 1.4 (dashed curve), were chosen for the shifting exponent, s, to illuminate the influence thereof on the obtained matching curve. The 'jump' in the value of the dependent variable, cf. Eq. (24), is evident.

Eq. (28) with a shifting exponent of 0.4 yields a fairly accurate prediction for k_v/k_∞ over the entire range of Slater–Reynolds numbers considered. Moreover, an overall qualitative improvement in prediction ability of the process is achieved by elimination of the discontinuity which results from application of Eq. (24). What is important to emphasise is that a single equation is obtained for prediction over the entire range of the independent variables. The expression not only correctly predicts the extremal values, but it also produces a curve that may be adjusted to closely fit the data. It is, however, evident from the present analysis that more careful, controlled experimentation with an individual fluid under different conditions will be needed. To arrive at a more accurate prediction of the shifter, s, it is recommended that experiments be tailored so as to specifically investigate the flow parameters in the transitional regime.

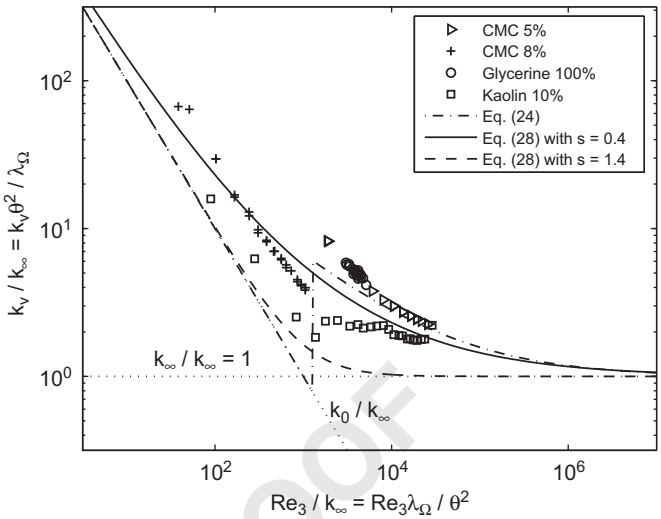

Fig. 2. Typical correlation of experimental data with the empirical two-constant model, Eq. (24), showing the 'jump' at $Re_3=10$, and the Churchill–Usagi matched solution as per Eq. (28).

4. Fluidised bed

A fluidised bed has a number of highly useful properties that may be utilised in industrial applications. Although the mechanism may be both physical and chemical in nature, the dominating attribute utilised in a specific industrial process, will determine its application (a broad classification of fluidised bed applications is given by Geldart, 1986). Experimental data was obtained from measurements performed on laboratory-scale fluidised beds. Upon analysis of the sets of collected data it became evident that asymptotes exist for some variable dependencies in the transition from packed- to fluidised bed. The transition between such asymptotes is governed, amongst others, by parameters such as particle size, particle size distribution, superficial gas velocity and bed height. Power addition to a power, s, of such asymptotes f_0 and f_∞, leads to a single correlating equation that is applicable over the whole range of flow rates.

4.1. Experimental procedure

The bed was contained in a cylindrical perspex tube with an inner diameter of 72 mm. Since the investigation was only concerned with the pressure drop across a specified section of the bed (i.e. between two pressure sensors), the porosity of the plate on which the bed was supported was irrelevant. It was only required not to allow particles to drop through into the antechamber and to function as a uniform gas distributor. To prevent particle entrainment the uppermost end of the containing perspex tube was covered with a porous paper cap and the bed illuminated from behind to allow easy visual detection of the onset of fluidisation.

The beds comprised glass powders, consisting of spherical glass particles, with a density of 2485 kg/m^3 and available in three different diameter-ranges: 100–200; 400–600; and 750−1000 μm. These particles all fall into Groups B and D according to the Geldart (1986) powder classification. Since the particles are manufactured they were assumed, for the sake of simplicity, to be perfectly spherical in shape and thus have a Waddell sphericity factor of

Please cite this article as: de Wet, P., et al., Application of power addition as modelling technique for flow processes: Two case studies. Chemical Engineering Science (2011), doi:10.1016/j.ces.2011.01.040

$\Psi = 1$ (Geldart, 1986). In all of the experiments performed the fluid used to fluidise the bed was air at ambient conditions, with a density of 1.2 kg/m^3 and viscosity of 1.78×10^{-5} N s/m^2. Air was pumped into the bed by a compressor and flow into the antechamber was controlled via a manual valve. A digital flow meter, situated between the valve and the antechamber, registered the fluid velocity. By using different gas velocities and only one particle diameter-range or a mixture of the particle diameter-ranges, the parameters of the experiment could be varied. Eight equidistantly spaced pressure taps were placed along the height of the bed and were connected to digital pressure sensors that measured the pressure (in mbar) at these fixed intervals within the bed. An experiment-specific software program was used with which the data from each sensor were recorded and written to file. The program, once calibrated, allowed for the interval between consecutive readings to be varied. A minimum of three runs were performed for each of the three different diameter-ranges mentioned above. A run consisted of a gradual increase in gas velocity up to and beyond fluidisation, followed by a gradual and controlled decrease to zero fluid flow. It was noted that hysteresis only became apparent if the bed was allowed a period of rest between consecutive fluidisations. Consequently, runs for a particular diameter-range were conducted in succession allowing the obtained pressure-values to be averaged. It is to this averaged data that the power addition was applied.

4.1.1. Determining the porosity of the packed bed

For each of the diameter-ranges an amount of powder was weighed and poured into the cylindrical perspex tube comprising the fluidised bed. Once inside the tube, the powders were briefly allowed to settle before commencing experimentation. By measuring the distance between the supporting porous plate at the base of the bed and the bed surface, the bulk volume, U_0, occupied by the powder (and hence that of the bed) could be calculated. Simple substitutions with, and algebraic manipulation of, the basic definitions for porosity, ε, and density, ρ, leads to an expression for the porosity (or bed voidage) in terms of known or easily measurable quantities, i.e.

$$\varepsilon = \frac{\rho_s - \rho_0}{\rho_s - \rho_f}. \tag{34}$$

In the idealised situation of an infinitely sized bed, the diameter of spherical particles would have no influence on the porosity of the bed. However, in the constrained bed found in small-scale experimental applications, the cross-sectional area of the bed will influence the packing of the particles. Conversely the diameter of particles thus impacts indirectly on the porosity of the bed by having an influence on the bulk volume (and thus the bulk density), as evident in the different porosities obtained for each of the diameter-ranges: 0.391, 0.368 and 0.362, respectively, as listed above.

4.2. Asymptotic dependencies

Three regimes are to be identified, namely the two regimes corresponding, respectively, to the physical conditions related to the two asymptotes f_0 and f_∞ and the change-over regime connecting the two. This latter regime surrounds the critical point, q_c, where the asymptotes meet. Of particular interest is the relation between the extent of the change-over regime surrounding the critical point and the shifting exponent s. In the present case of onset of fluidisation the change-over between the packed bed condition and the fluidised state is fairly abrupt leading to a relatively high value of s. These effects will be discussed in the following section.

4.2.1. Lower asymptote

Before the onset of fluidisation, the bed may be regarded as a packed bed or porous medium consisting of spherical particles. To describe the pressure drop of Newtonian flow through such a structure, the Ergun equation (e.g. Bird et al., 1960) has proven to be satisfactory in most applications as is evident from its extensive utilisation in chemical engineering. In the original Ergun equation, which is incidentally already a special case of power addition with shifter, $s=1$,

$$\frac{\Delta p}{H} = M\frac{(1-\varepsilon)^2}{\varepsilon^3}\frac{\mu q}{D_p^2} + N\frac{1-\varepsilon}{\varepsilon^3}\frac{\rho_f q^2}{D_p}. \tag{35}$$

The values of coefficients M and N were acquired experimentally and reported as 150 and 1.75, respectively (Bird et al., 1960; Niven, 2002; Churchill, 1999). Here Δp denotes the finite pressure difference (measured in the streamwise direction of fluid flow), H the bed height, q the magnitude of the superficial velocity of the traversing fluid and D_p the spherical particle diameter. In their paper Du Plessis and Woudberg (2008), compare the RUC (representative unit cell) model to the Ergun equation for the description of Newtonian flow through a packed bed of uniformly sized spherical granules and find the agreement to be satisfactory. The cubic RUC contains a solid, cubic granule which resembles the average solid geometry of the granular porous medium. The choice, in this paper, of their RUC model to describe the asymptotic relation at small values of the independent variable is due to the fact that it is adaptable to different physical situations, whereas the Ergun equation is empirically based and the coefficients, M and N, will thus vary according to the situation to which it is applied. Furthermore the RUC model permits the usage of the average bed porosity and is applicable over both the entire porosity and laminar Reynolds number ranges. The work of Du Plessis and Woudberg (2008) allows one to purge Eq. (35) of some of its empirical elements. Their pore-scale analysis of interstitial flow conditions leads to the following expression of coefficients:

$$M = \frac{25.4\varepsilon^3}{(1-\varepsilon)^{2/3}(1-(1-\varepsilon)^{1/3})(1-(1-\varepsilon)^{2/3})^2}, \tag{36}$$

and

$$N = \frac{\varepsilon^2 c_d}{2(1-(1-\varepsilon)^{2/3})^2}, \tag{37}$$

with c_d a form drag coefficient. They thus succeed in rewriting Eq. (35) such that it is not limited by the range of porosities used. Here the particle Reynolds number, Re_p, is defined as

$$Re_p \equiv \frac{\rho_f q D_p}{\mu}. \tag{38}$$

The spherical particle diameter, D_p, is assumed to be equal to the linear dimension d_s of the solid cube of the granular RUC model. As in Du Plessis and Woudberg (2008) the value of the form drag coefficient, c_d in Eq. (37), was taken to be 1.9, presenting the most empirical aspect of the procedure.

4.2.2. Upper asymptote

As noted by Geldart (1986), the pressure drop across a fluidised bed, given by

$$\Delta p = \frac{m_0 g}{A_c} = \frac{\rho_0 U_0 g}{A_c} = \rho_0 g H, \tag{39}$$

is the only parameter that can be predicted with accuracy, since at all times during fluidisation the downward force, i.e. the weight of the bed, $m_0 g$, is balanced by the upward force, $\Delta p A_c$. Here m_0 denotes the bulk mass, ρ_0 the bulk density, U_0 the bulk volume, g acceleration due to gravity (taken as 9.81 m/s^2) and A_c the cross-sectional area of the bed. Division of Eq. (39) by the bed height

Please cite this article as: de Wet, P., et al., Application of power addition as modelling technique for flow processes: Two case studies. Chemical Engineering Science (2011), doi:10.1016/j.ces.2011.01.040

yields

$$\frac{\Delta p}{H} = \frac{m_0 g}{A_c H} = \frac{\rho_0 U_0 g}{A_c H} = \rho_0 g, \tag{40}$$

which forms the upper limiting asymptote.

4.3. Power addition of asymptotes

The original Ergun equation, Eq. (35), was obtained through simple addition of the Blake–Kozeny and Burke–Plummer equations (e.g. Bird et al., 1960; Niven, 2002), the former being a Darcy-type equation predominating in the regime where $Re_p \to 0$ and the latter dominating in the Forchheimer regime. If power addition is used to match the asymptotic conditions, i.e. Eqs. (35) and (40) are combined, a single correlative equation,

$$\frac{\Delta p}{H} = \left[\left(M\frac{(1-\varepsilon)^2}{\varepsilon^3}\frac{\mu q}{D_p^2} + N\frac{1-\varepsilon}{\varepsilon^3}\frac{\rho_f q^2}{D_p}\right)^s + (\rho_0 g)^s\right]^{1/s}, \tag{41}$$

is obtained for the pressure drop over the bed. Here coefficients M and N are as expressed in Eqs. (36) and (37), respectively.

4.3.1. Critical point and shifting exponent

As discussed in Section 2.4 the critical point of the matching curve is the value of the independent variable at which the asymptotes meet. To determine this value for the case of the fluidised bed, the two asymptotes are set equal, i.e.

$$M\frac{(1-\varepsilon)^2}{\varepsilon^3}\frac{\mu q}{D_p^2} + N\frac{1-\varepsilon}{\varepsilon^3}\frac{\rho_f q^2}{D_p} = \rho_0 g, \tag{42}$$

which yields a quadratic equation in q. Let q_c denote the value of the independent variable at which the asymptotes meet. Solving $q = q_c$ in Eq. (42) yields

$$q_c = \frac{M}{N}\frac{\mu}{2\rho_f D_p}(1-\varepsilon)\left[-1 \pm \sqrt{1 + \frac{N}{M^2}\frac{\varepsilon^3}{(1-\varepsilon)^3}\frac{4\rho_0\rho_f g D_p^3}{\mu^2}}\right]. \tag{43}$$

Since the second term inside the square root of Eq. (43) is greater than or equal to zero and $q_c \geq 0$, it follows that the negative root may be disregarded. Substitution of this q_c-value into Eq. (41) will yield the function value at the intersection of the asymptotes. It is also worth noting that once the pressure drop created by the fluid flow becomes sufficient to support the weight of the bed, fluidisation will take an onset. This is referred to as the point of *incipient fluidisation* and the corresponding superficial velocity of the fluid as the minimum fluidisation velocity, q_{mf}. Seeing as the upper limiting asymptote predominates in the composition of the matched solution beyond the critical point, this point of intersection is the threshold value of the superficial velocity at which fluidisation will occur. The value found by Eq. (43) will thus be a theoretical prediction of the minimum velocity required to fluidise the bed, i.e. $q_{mf} = q_c$.

The experimental data was traversed in search of the q_c-value matching the theoretically predicted value of the critical point, as expressed by Eq. (43), most closely. From Eq. (43) it is clear that the diameter of the particle impacts on the value of q_c, and thus on $f_c = f\{q_c\}$, Eq. (41). The latter in turn has a direct influence on the value of s, as calculated by Eq. (20). In the format of Eq. (41), with $\Delta p/H$ the dependent and q the independent variable, the relation shows a decreasing dependence as the superficial velocity grows. Furthermore, both the functions at the extremal values are presumed to form upper bounds on the value that the pressure drop may take. Hence, it is expected that the plot should be qualitatively analogous to the case outlined in Section 2.2.2 and a negative value of the shifting exponent is to be expected. Indeed, this turns out to be the case.

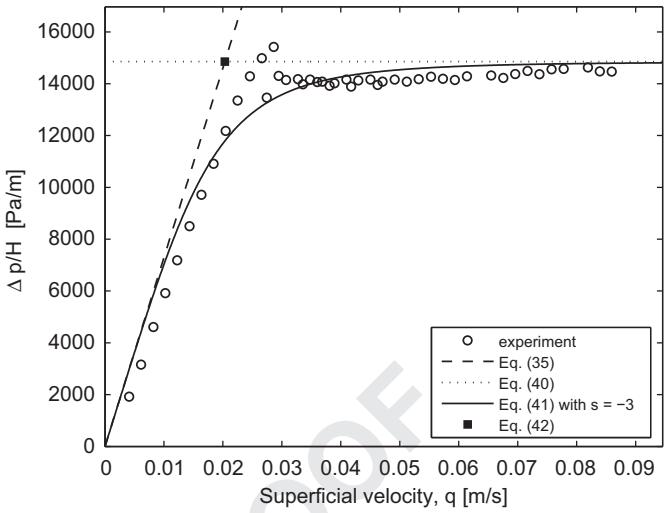

Fig. 3. Experimental pressure drop data against superficial velocity for particles in diameter-range 100−200 μm with curve-fitting by power addition.

Once the experimental value of the pressure drop at the critical point, $f_c = f\{q_c\}$, for each of the diameter-ranges had been determined by the method discussed above, the value of the shifter was calculated with the aid of Eq. (20) which yielded a value of −3. In these calculations, that is Eqs. (35), (41) and (43), the median particle diameter (as determined by sieve-analysis) of each range was used. In Fig. 3 the experimental data for the 100−200 μm diameter-range is plotted along with the result obtained when applying Churchill and Usagi's method (Churchill and Usagi, 1972, 1974; Churchill, 1988, 2001) of power addition, the specific instance of which is given by Eq. (41). Similar plots may also be constructed for the 400–600 and 750−1000 μm particle diameter-ranges. The figure also indicates the asymptotes applicable below (Eq. (35)) and beyond (Eq. (40)) the point of fluidisation as well as its location (i.e. the critical point, q_c, as per Eq. (43)).

As mentioned in Section 3.3, it should be remembered that the datum point chosen upon traversal of the experimental data may be a poor choice. Establishing the s-value purely based on this principle may lead to erroneous results and hence the value of visual inspection should never be underestimated (besides, the method is empirical). As Churchill and Usagi notes Churchill and Usagi, 1972, 1974; Churchill, 1974, 1988) the solution is relatively insensitive to small changes in s and hence the values for the shifting exponent with the aid of Eq. (20) were rounded in each of the corresponding figures. Alternatively the predictive curve could have been manually adjusted until satisfactory visual correlation with the data had been achieved, whence a value would be assigned to s.

Fig. 3 shows that, using a shifting exponent of −3, the values predicted by Eq. (41) correspond well with the experimental data in the two asymptotic extremities of the dependent variable. However, in the transition regime Eq. (41) predicts a gradual change-over whereas the experimental data exhibits a much more abrupt transition, with some data points even crossing the upper limit (see Fig. 3). This discrepancy between predicted and measured values is addressed in the next section.

4.3.2. Crossing of the upper asymptote

In Section 2.3 a method was outlined to construct a (postulated) dependence should the collected data cross the upper limiting asymptote.

Referring to Fig. 3 it is evident from the experimental data that this is the case for particles within the diameter-range 100−200 μm.

Please cite this article as: de Wet, P., et al., Application of power addition as modelling technique for flow processes: Two case studies. Chemical Engineering Science (2011), doi:10.1016/j.ces.2011.01.040

This phenomenon is, according to Geldart (1986) and Davidson and Harrison (1963), caused by the wedging action within the bed and cohesion between the particles and is prevalent in beds composed of Group B particles (into which this diameter-range resorts).

Making use of the functional form suggested by Eq. (15), the dependence

$$\frac{\Delta p}{H} = \rho_0 g\left[1+\left(\frac{q_A}{q}\right)^{\alpha}\right], \tag{44}$$

was postulated to represent behaviour of the bed in the upper limit of the superficial velocity. Here q_A is equivalent to the arbitrary constant, x_A of Eq. (15) and α is an arbitrary exponent (see Section 2.3), and, respectively, determine the point of intersection and curvature of the postulated function with Eqs. (35)–(37). The values of both these variables were chosen by trial and error, with the former being selected relative to the critical point, calculated in Eq. (43), as $q_A = 1.2q_c$, and the latter as $\alpha = 5$. Since both q_A and α influence the form of the function postulated for the upper limit they may essentially be regarded as turning parameters with which the postulated function is 'shaped'. These constants are however assigned values before power addition is effected. The RUC model, as per Eqs. (35)–(37), was kept as representative of the lower asymptote. After applying power addition to the constituent terms in the functional expression and some rearrangement, the pressure drop across the bed may be expressed as

$$\frac{\Delta p}{H} = \frac{\zeta_0\{q\}\zeta_\infty\{q\}}{(\zeta_0\{q\}^s+\zeta_\infty\{q\}^s)^{1/s}}. \tag{45}$$

Here $\zeta_0\{q\}$ is the functional dependence of the pressure drop on the superficial velocity in the lower limit as given by Eq. (35) and $\zeta_\infty\{q\}$ as per Eq. (44).

As in Fig. 3 the pressure drop was plotted against the superficial velocity. In Fig. 4 the outcome of plotting the matched curve, Eq. (45), against the collected data is demonstrated. Once again, similar plots may be drawn for the 400–600 and 750−1000 μm particle diameter-ranges. It is important to note that the asymptotes need not necessarily be straight lines, for instance, the quadratic nature of the RUC model in the lower asymptote only becomes apparent with the larger particle diameters (750−1000 μm) where an increased superficial velocity is required before fluidisation takes an onset. In Fig. 4, $q_A = 1.2q_c$, $\alpha = 5$ and $s = 2$ were substituted into the functional relation given in Eq. (45). Noteworthy is the fact that in Fig. 3 the value of the shifting exponent is negative, whereas $s > 0$ in Fig. 4. Rearrangement, as outlined in Section 2.2.2, Eq. (13), was performed to the constituent equations to obtain Eq. (45) and hence a positive value for s. The degree of agreement between the experimental data and predictive curve is a satisfactory result. Also shown in this Fig. 4 is the original two asymptotic relations, Eqs. (35) and (40), as well as the postulated function, described by Eq. (44).

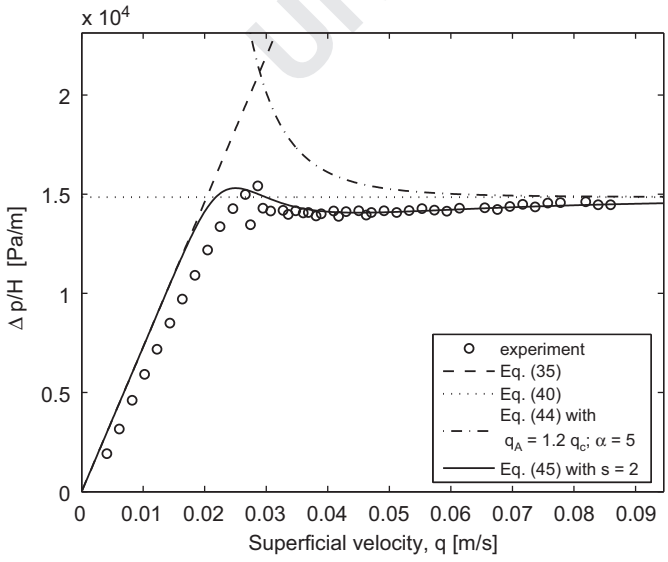

Fig. 4. Curve-fitting by power addition with a postulated function for the upper limiting dependency to enable crossing of the upper extremal value. Particles in diameter-range 100−200 μm.

5. Discussion

The method of power addition, formalised by Churchill and Usagi (1972), succeeds, through simple exponentiation of the constituent terms, in adjusting the solution so as to more closely trace the experimental or computational data. The procedure should not be regarded as a trick; rather linear addition of asymptotic functions should be regarded as a special case of power addition with a shifting exponent equal to unity. Prior knowledge of the functional behaviour in at least one of the limits makes the direct application of the proposed method possible. Should, however, only the limiting value be known at one of the extremities an empirical expression may be postulated, in which case a power function is pertinent. The uncomplicated form of a power function makes it a satisfactory choice and is in tune with the method's underlying philosophy of simplicity. Although the routine has not yet been proven to accurately describe the relative behaviour of the different parameters during a transfer process, it may be argued to be appropriate, since the rate of change between the two asymptotes can be adjusted to fit experimental readings. For instance, the higher the (absolute) value of the shifter-exponent, s, the more abrupt the change-over between the two asymptotic processes. Furthermore, irrespective of the rate at which the change-over occurs, it will be a smooth transition as is expected for the cross-over from one continuum process to another. The method thus ensures that the solution is correct at the extreme values and allows careful adjustment in the transitional regime. This is often not the case with polynomial fitting. It may also be argued that the leading coefficients and constants of a polynomial (even if unity) would each require a physical interpretation or validation, which is a drawback of a polynomial fitting technique.

In the examined cases in this study, and the various examples listed in the literature by Churchill et al. (Churchill and Usagi, 1972, 1974; Churchill, 1974, 1988, 2001), powered addition appears to be favoured over the introduction of *ad hoc* curve-fitting or bridging functions which might introduce unwanted jumps. Thus, although primarily a curve-fitting exercise, this procedure leads to better physical modelling since the only 'tuneable' parameter is the shifter-exponent, s. Adjusting its value does not change the value of the asymptotic conditions and leaves the double-asymptote character of the transfer process intact. In certain instances the shifting exponent may be linked to specific parameters of the process. The choice of s for both the cases of this study was however made purely by inspection of the collected data without any physical justification.

Due to the sensitivity of the matched curve to changes in the shifter, s, in the vicinity of intersection of the asymptotes, it is recommended that experiments be designed so as to focus on this area. More specifically, in performing an experiment it is advantageous to arrange the physical conditions in such a manner that the independent variable is in close proximity of the critical point. Should the experimental values of the dependent variable at the critical point be known, a good indication of the value of the

Please cite this article as: de Wet, P., et al., Application of power addition as modelling technique for flow processes: Two case studies. Chemical Engineering Science (2011), doi:10.1016/j.ces.2011.01.040

shifting exponent may be obtained analytically. It is however important to keep in mind that, since the method is empirical in nature, an exact solution is not obtained and therefore the potential benefit of visual inspection and evaluation on the result should not be disregarded (visual inspection by trial and error adjustment often leads to a better value assignment of the shifting exponent). As noted by Churchill and Usagi (1972) the matched curve is relatively insensitive to small variations in s and the required accuracy should be determined by considerations such as the process involved, tunability of other parameters and allowable error-margin.

The main advantages of the method are that a singular functional dependence of the independent variable upon the dependent variable is established over the entire range of the latter. The inherent simplicity of the method suggests that in such a curve-fitting exercise the greater deal of effort should be exerted in determination of the asymptotes, the value of the exponent, s, and possible relation of the latter to some quantifiable parameter.

6. Conclusion

A single predictive equation is proposed for predicting the pressure drop over a straight-through diaphragm valve which serves as an improvement on an existing empirical set of equations. The latter involves a discontinuity in the pressure drop in the transition regime of superficial flow velocities, whereas the equation proposed in this study ensures a smooth change-over as the Slatter–Reynolds number increases.

In the second case study a single equation is proposed for predicting the pressure drop over a fluidised bed. This equation accounts for both the packed bed state at low superficial velocities and the fluidised state at higher superficial velocities. It was illustrated how the characteristic 'hump', often exhibited in experimental pressure drop values due to particle interlocking, can be accounted for in the predictive equation with promising results.

Although the authors have not yet succeeded in quantifying the power, s, for the cases discussed in this paper, and despite the lack of an obvious physical meaning being attached to the parameter at this stage, it was shown that the shifting exponent is closely linked to the changeover rate between the limiting, asymptotic solutions. Application of the approach to two diverse continuum processes, often found in chemical engineering, were discussed to illustrate the wide utilisation possibilities of the method.

References

Bird, R.B., Stewart, W.E., Lightfoot, E.N., 1960. Transport Phenomena. John Wiley & Sons, Inc., New York, USA.

Churchill, S.W., 1974. The Interpretation and Use of Rate Data: The Rate Concept. McGraw-Hill, New York, USA.

Churchill, S.W., 1988. Derivation, selection, evaluation and use of asymptotes. Chemical Engineering and Technology 11, 63–72.

Churchill, S.W., 1999. Similitude: dimensional analysis and data correlation. In: Kreith, F. (Ed.), Mechanical Engineering Handbook. CRC Press LLC, Boca Raton, USA, pp. 28–43 (Chapter 3).

Churchill, S.W., 2001. Correlating equations for transitional behavior. Industrial and Engineering Chemistry Research 40, 3053–3057.

Churchill, S.W., Usagi, R., 1972. A general expression for the correlation of rates of transfer and other phenomena. American Institute of Chemical Engineers Journal 18 (6), 1121–1128.

Churchill, S.W., Usagi, R., 1974. A standardized procedure for the production of correlations in the form of a common empirical equation. Industrial and Engineering Chemistry, Fundamentals 13 (1), 39–44.

Davidson, J.F., Harrison, D., 1963. Fluidised Particles. Cambridge University Press, London, UK.

De Wet, P.D., 2010. Powered addition as modelling technique for flow processes. Master's Thesis, University of Stellenbosch, Stellenbosch, South Africa.

De Wet, P.D., Halvorsen, B.M., Du Plessis, J.P., 2009. Powered addition applied to the fluidisation of a packed bed. In: Mammoli, A.A., Brebbia, C.A. (Eds.), Computational Methods in Multiphase Flow V, 15–17 June. WIT Press, Southampton, UK, pp. 431–441.

Du Plessis, J.P., Woudberg, S., 2008. Pore-scale derivation of the Ergun equation to enhance its adaptability and generalization. Chemical Engineering Science 63 (1), 2576–2586.

Fester, V.G., Kazadia, D.M., Mbiya, B.M., Slatter, P.T., 2007. Loss coefficients for flow of Newtonian and non-Newtonian fluids through diaphragm valves. Chemical Engineering Research and Design 85 (9), 1314–1324.

Geldart, D., 1986. In: Geldart, D. (Ed.), Gas Fluidization Technology. John Wiley & Sons, Inc., Chichester, UK, pp. 1–54 (Chapters 1–3).

Mbiya, B.M., 2007. Predicting pressure losses in straight-through diaphragm valves. Ph.D. Thesis, Cape Peninsula University of Technology, Cape Town, South Africa.

Mbiya, B.M., Fester, V.G., Slatter, P.T., 2009. Evaluating resistance coefficients of straight-through diaphragm control valves. The Canadian Journal of Chemical Engineering 87 (5), 704–714.

Myles, K., 2000. Knowing More About Valves. K Myles and Associates cc, Northcliff, Johannesburg, South Africa.

Niven, R.K., 2002. Physical insight into the Ergun and Wen Yu equations for fluid flow in packed and fluidised beds. Chemical Engineering Science 57, 527–534.

Slatter, P.T., 1994. Transitional and turbulent flow of non-newtonian slurries in pipes. Ph.D. Thesis, University of Cape Town, Cape Town, South Africa.

Slatter, P.T., 1999. The role of rheology in the pipelining of mineral slurries. Mineral Processing and Extractive Metallurgy Review 20 (1), 281–300.

Streeter, V.L., 1966. Fluid Mechanics, fourth ed. McGraw-Hill, New York, USA.

Please cite this article as: de Wet, P., et al., Application of power addition as modelling technique for flow processes: Two case studies. Chemical Engineering Science (2011), doi:10.1016/j.ces.2011.01.040